AD-A118 610 VIRGINIA POLYTECHNIC INST AND STATE UNIV BLACKSBURG --ETC F/G 13/2
FEASIBILITY OF COMPUTING RESIDUAL DISPLACEMENTS IN RUNWAYS AND --ETC(U)
APR 82 L C RUDE AFOSR-81-0102

UNCLASSIFIED AFOSR-TR-82-0669 NL

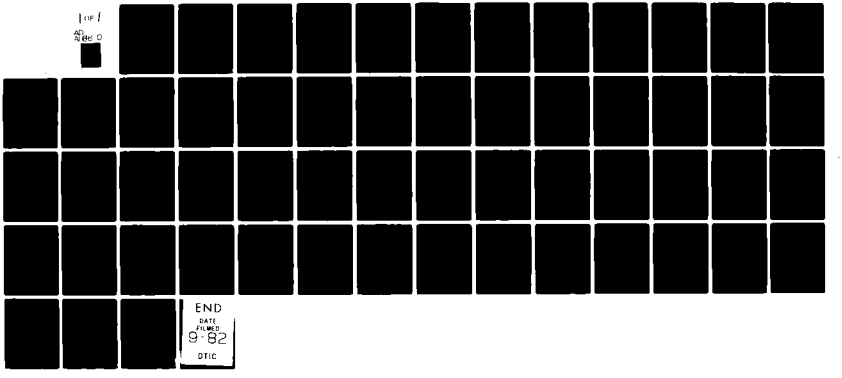

END
DATE FILMED
9-82
DTIC

(8)

UNCLASSIFIED
SECURITY CLASSIFICATION OF THIS PAGE (When Data Entered)

REPORT DOCUMENTATION PAGE		READ INSTRUCTIONS BEFORE COMPLETING FORM
1. REPORT NUMBER AFOSR-TR- 82-0869	2. GOVT ACCESSION NO. AD-A118610	3. RECIPIENT'S CATALOG NUMBER
4. TITLE (and Subtitle) FEASIBILITY OF COMPUTING RESIDUAL DISPLACEMENTS IN RUNWAYS AND CRATER REPAIRS		5. TYPE OF REPORT & PERIOD COVERED FINAL 25 Mar 81 - 6. PERFORMING ORG. REPORT NUMBER
7. AUTHOR(s) LAWRENCE C RUDE		8. CONTRACT OR GRANT NUMBER(s) AFOSR-81-0102
9. PERFORMING ORGANIZATION NAME AND ADDRESS VIRGINIA POLYTECHNIC INSTITUTE AND STATE UNIVERSITY DEPARTMENT OF CIVIL ENGINEERING BLACKSBURG, VA 24061		10. PROGRAM ELEMENT, PROJECT, TASK AREA & WORK UNIT NUMBERS 61102F 2307/D9
11. CONTROLLING OFFICE NAME AND ADDRESS AIR FORCE OFFICE OF SCIENTIFIC RESEARCH/NA BOLLING AFB, DC 20332		12. REPORT DATE April, 1982 13. NUMBER OF PAGES 57
14. MONITORING AGENCY NAME & ADDRESS(if different from Controlling Office)		15. SECURITY CLASS. (of this report) UNCLASSIFIED 15a. DECLASSIFICATION/ DOWNGRADING SCHEDULE

16. DISTRIBUTION STATEMENT (of this Report)

Approved for Public Release; Distribution Unlimited.

17. DISTRIBUTION STATEMENT (of the abstract entered in Block 20, if different from Report)

Approved for Public Release; Distribution Unlimited.

18. SUPPLEMENTARY NOTES

19. KEY WORDS (Continue on reverse side if necessary and identify by block number)

Civil Engineering	Crater Repair
Air Field	Computer Code
Pavements	Finite Element

20. ABSTRACT (Continue on reverse side if necessary and identify by block number)

The purpose of this study was to determine the feasibility of computing residual displacements in runways and crater repairs under repeated aircraft loadings. This report presents a methodology for computing residual displacements that is economical and easy to use. It also contains a literature review and a presentation of a second procedure to compute residual displacements. Sample calculations were done to illustrate the first procedure and the results compared favorably with previously published test data. The limitations of the second procedure were also discussed.

DD FORM 1 JAN 73 1473 EDITION OF 1 NOV 65 IS OBSOLETE

UNCLASSIFIED
SECURITY CLASSIFICATION OF THIS PAGE (When Data Entered)

AFOSR-TR- 82-0669

Feasibility of Computing Residual Displacements in Runways and Crater Repairs

by

Lawrence C. Rude
Assistant Professor
Department of Civil Engineering
Virginia Polytechnic Institute and State University
Blacksburg, Virginia

Conditions of Reproduction

Reproduction, translation, publication, use and disposal in whole or in part by or for the United States Government is permitted.

AIR FORCE OFFICE OF SCIENTIFIC RESEARCH (AFSC)
NOTICE OF TRANSMITTAL TO DTIC
This [illegible] has been reviewed and is approved [illegible] IAW AFR 190-12.
Distribution unlimited.
MATTHEW J. KELLY
Chief, Technical Information Division

TABLE OF CONTENTS

FEASIBILITY OF COMPUTING RESIDUAL DISPLACEMENTS IN RUNWAYS AND CRATER REPAIRS

by

Lawrence C. Rude
Assistant Professor
Department of Civil Engineering
Virginia Polytechnic Institute and State University
Blacksburg, Virginia

ABSTRACT

The purpose of this study was to determine the feasibility of computing residual displacements in runways and crater repairs under repeated aircraft loadings. This report presents a methodology for computing residual displacements that is economical and easy to use. It also contains a literature review and a presentation of a second procedure to compute residual displacements. Sample calculations were done to illustrate the first procedure and the results compared favorably with previously published test data. The limitations of the second procedure were also discussed.

CHAPTER 1

Scope and Concept for Computing Residual Displacements

Introduction

The purpose of this report is to present the results of a feasibility study for computing the residual displacements in airport pavements and crater repairs. The study emphasized the application of the finite element method of analysis with the incorporation of non-linear behavioral laws to represent the base and subbase material of the pavement structure. The report consists of three sections. The first section presents the scope and concept of the study. Section two presents a brief literature review and background information. Section three is a presentation of several proposed procedures along with sample calculations. Limitations and further research for each procedure are also presented. In general, the report concludes that there does exist an economical and feasible procedure for computing residual displacements.

Scope and Concept of a Method for Computing Residual Displacements

Concept

Airport pavements are subjected to many different types of load applications. Runways are subjected to high-speed takeoff and landings, i.e., dynamic and impact loading from many different types of aircraft. Taxiways handle aircraft under static loading conditions. High-speed runway exits handle dynamically applied wheel loadings.

An idealized analysis procedure that used the finite element method is presented below. This procedure presupposes that capital costs do

not hinder testing of pavement materials or computer operating time, and the computer core size does not limit the size of the finite element mesh. First, the dynamic and static constitutive (stress-strain) properties of the pavement materials would be determined. Secondly, a three dimensional finite element grid could be constructed. Lastly, the actual plane movements, including takeoffs, landings and taxiing, could be simulated in the time domain, taking into account the fact that planes traffic at different positions along the length of the runways and along different positions with respect to the center line of the runway. The computer would actually simulate the landing, takeoffs and taxiing in three dimensions with aircraft moving simultaneously throughout various portions of the airport. The computer would automatically switch from dynamic constitutive relations to static constitutive relations depending on the velocity of the aircraft.

The hypothetical description of a mythical computer program could be achieved on perhaps a few computers in the country. Such a program would not, however, be possible to operate on a majority of the mainframe computers at most government installation or universities. Such a program may be the state of the art in the near future, but this is not consistent with the current state of the art exposed during the present research project. The procedure developed during the study was well within the financial limitations and computer size limitations as they presently exist.

Current finite element analyses of airport pavements include axisymmetric, plane strain, and prismatic solid representation. Elastic layer theories, mats on a Winkler subgrade and visco-elastic solutions are also currently used. Most computation procedures handle a one-time

loading of the pavement system. Many procedures use a resilient modulus so that the response during one of the many load applications can be analyzed. None of the current programs had the capacity to handle multiple application of cyclic loadings.

Pavement materials include concrete, bituminous asphaltic concrete, gravel subgrades and soil subbases. These materials actually have a nonlinear relation between stress and strain; that is, when a load is applied and then removed, the material will not return to its initial position. The material accumulates a permanent strain or set. A hypothetical stress-strain diagram is shown in Figure 1. The loading and unloading path are indicated as well as the permanent strain.

When a load is applied to a pavement material and removed many times, as occurs due to traffic applications, the permanent strain accumulates leaving a permanent or residual displacement in the pavement. Such ruts are often visible in unpaved roads or in bituminous highway pavements. The permanent strains usually accumulate rapidly during the first few applications of the load. After repeated applications, the accumulated set strain will either reach a limiting value or will undergo a rapid increase due to a fatigue type failure. An intermediate case where the strains increase according to a prescribed function is also possible. Figure 2 illustrates these behavioral patterns. Fatigue failures have been discovered to be related to the magnitude of stress application as compared to ultimate strength of the material. Some highway materials also exhibit a creep behavior.

In laboratory testing studies, many investigators have been able to relate the accumulated set strain to the set strain produced during the first loading cycle. In general the accumulated set strain, ε_r, is a

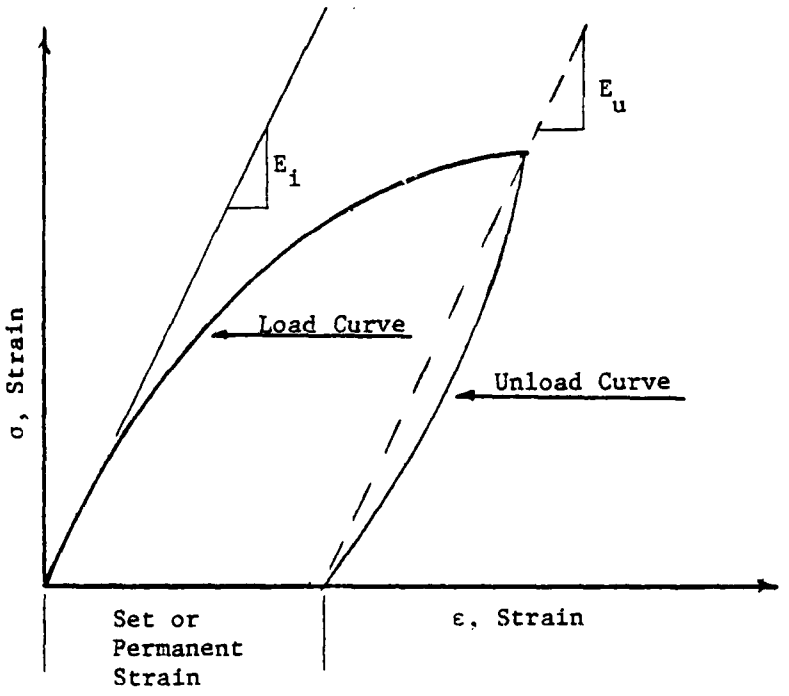

Figure 1. Stress-Strain Curve for Non-Linear Material

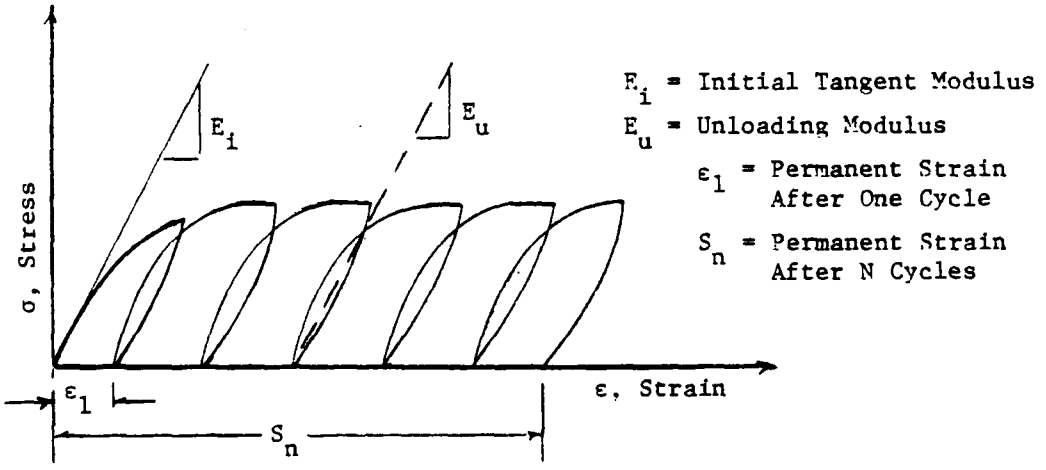

Figure 2. Cyclic Loading and Unloading for a Non-Linear Material

function of the number of loading N, the ratio of the stress applications, $\Delta\sigma$, to the ultimate strength σ_1, confining pressure, σ_3, and the first set strain, ε_1,

$$\varepsilon_r = F(\varepsilon_1, \Delta\sigma/\sigma_1, \sigma_3, N) \tag{1}$$

Compositional changes also affect the accumulated strain relationships.

The existing finite element programs could be slightly modified to calculate the permanent strain after the first cycle. The accumulated set strains for each element could then be calculated using Equation 1 and the total surface settlement Δh could be calculated by summing the change of height of each element, or

$$\Delta h = \sum_{i=1}^{\text{No. of element}} \varepsilon_{r,i} * h_i \tag{2}$$

where $\varepsilon_{r,i}$ is the accumulated set strain for each element and h_i is the height of each element. It is proposed that programs use non-linear constitutive laws to represent the material behavior. Linear constitutive laws are valid if appropriate engineering judgment is exercised in selecting the secant or tangential material modulus to approximate the non-linear behavior. As will be shown later, the initial strain finite element procedure can also be used to calculate permanent displacements.

Scope

Equation 2 represents the current concept described in the literature and was found to be the most feasible procedure most easily adoptable for computing residual displacements. It was the scope of this project to compare the application of this concept with published data

regarding rut accumulations and permanent deflections in bomb crater repairs and airport pavements. The use and the problems of using the initial strain procedure were also studied.

CHAPTER II

Background Information

Introduction

This section of the report provides a summary of some of the pertinent literature that was reviewed. The section is written in the chronological order of the development of the various ideas regarding the analysis of pavement systems and the accumulation of permanent deflections.

Literature Review

Ahmed and Larew (1962) publish the results of static and repeated load triaxial testing on three types of subgrade soils. These soils were a limestone residual silty-clay, a sandy clay, and a micaceous silt. All their testing was done with a single confining pressure of 10 psi. Duplicate samples were used for each soil. The average peak deviator stresses at static failure were determined for each soil, $\Delta\sigma_s$. A series of repeated load tests were run on each soil where the repeated deviator stress, $\Delta\sigma_r$, was held at certain ratios of the static ultimate deviator stress. Studies were also done to show the effects of water content, density and compactive effort.

The results of the study showed that, for the ratio of the dynamic deviator stress to the ultimate static dewater stress, $\Delta\sigma_r/\Delta\sigma_s$, below a critical level, the deformations reached a limiting value after a certain number of load applications. For a $\Delta\sigma_r/\Delta\sigma_s$ ratio above a critical value, a greater number of repetitions would increase the rate of deformation per load application and the sample would fail after a

certain number of load applications. Figure 3 illustrates these results.

Hardin (1971) reports the results of using specially designed equipment for determining shear stress relations of soil. The 1971 report presented a model for a silty sand and a silty clay. In 1972 and 1973, the model was applied to additional soils and gravel.

The model relates the sharing stress, τ, to the shearing strain, γ, using a secant shearing modulus G_s. See Figure 4. G_s was expressed as a hyperbolic equation as $G_s = G_{max}/(1+\gamma_h)$ where G_{max} was the maximum or initial tangent shearing modulus, and δ_h was the hyperbolic shear strain,

$$\gamma_h = \frac{\gamma}{\gamma_r}\left[1 + \frac{a}{\exp(\gamma/\gamma_r)}\right] \qquad (3)$$

where δ_r is the reference shear strain and a is an experimentally determined parameter.

The reference shear strain, γ_r, was defined as the ratio of the maximum shearing stress, τ_{max} to G_{max}. The advantage of Hardin's model was that the results of many different strength tests could be non-dimensionalized in terms of the reference strain as shown in Figure 5. The model was related experimentally to such characteristics as soil type, void ratio, plastic index, degree of saturation, rate of loading, and number of loading cycles.

Computer programs using Hardin's soil model employ an iterative scheme to represent the non-linear soil behavior. During each iteration, a stiffness matrix is formed and nodal displacements are computed. The nodal displacements are used to calculate element stresses and strains. At the end of each iteration the shear modulus of the soil

$$\left(\frac{\Delta\sigma_r}{\Delta\sigma_s}\right)_1 > \left(\frac{\Delta\sigma_r}{\Delta\sigma_s}\right)_2 > \left(\frac{\Delta\sigma_r}{\Delta\sigma_s}\right)_3 > \left(\frac{\Delta\sigma_r}{\Delta\sigma_s}\right)_4$$

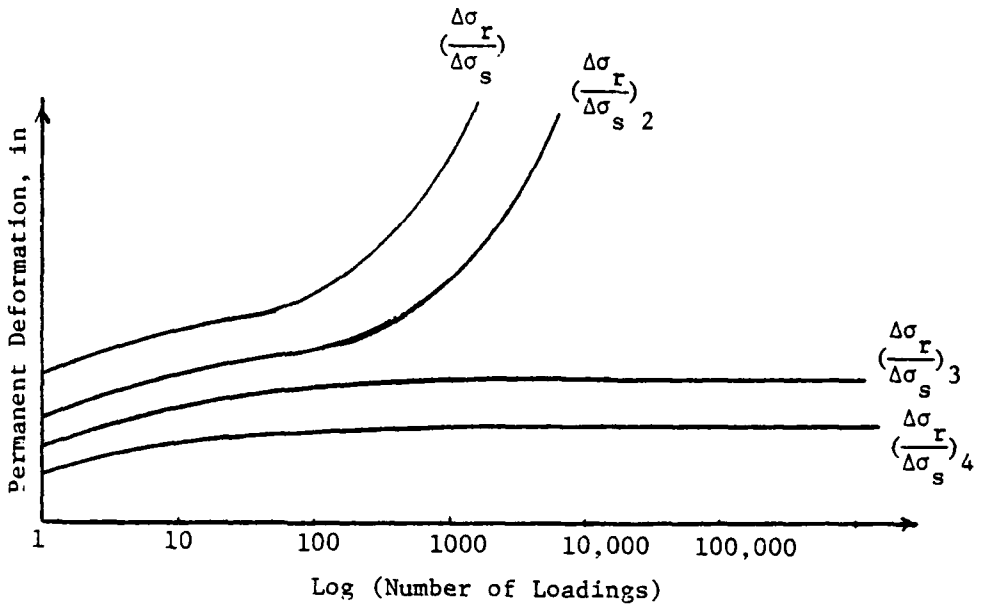

Figure 3. Typical Results from Ahmed and Larew (1962)

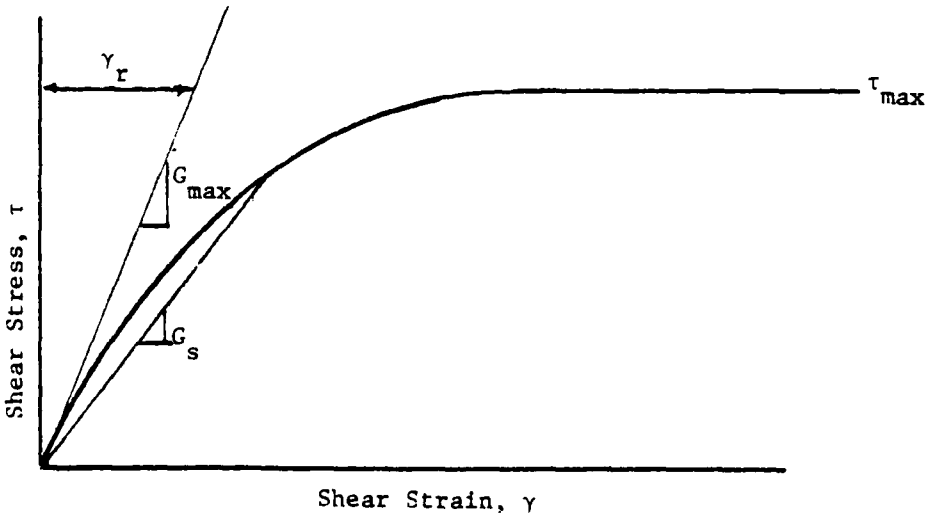

Figure 4. Hardin's (1971) Simple Shear-Stress Relationship

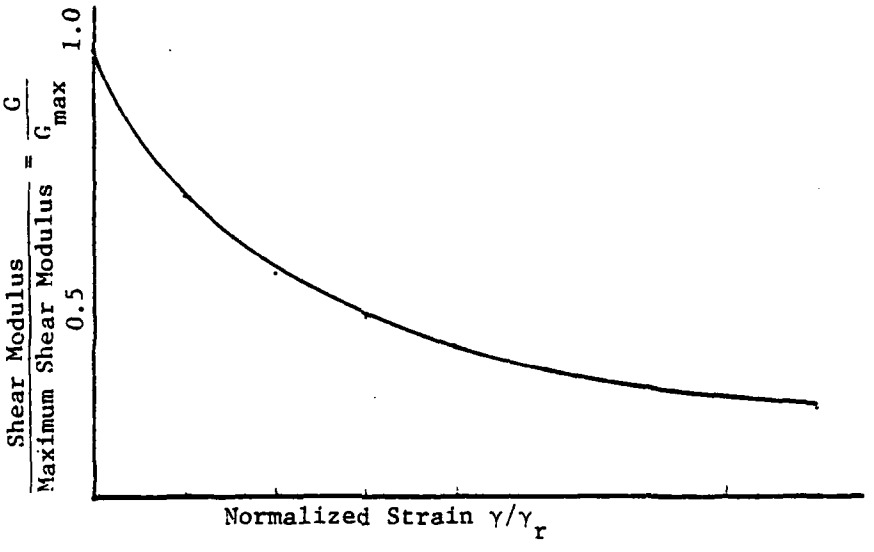

Figure 5. Hardin's (1971) Hyperbolic Soil Model

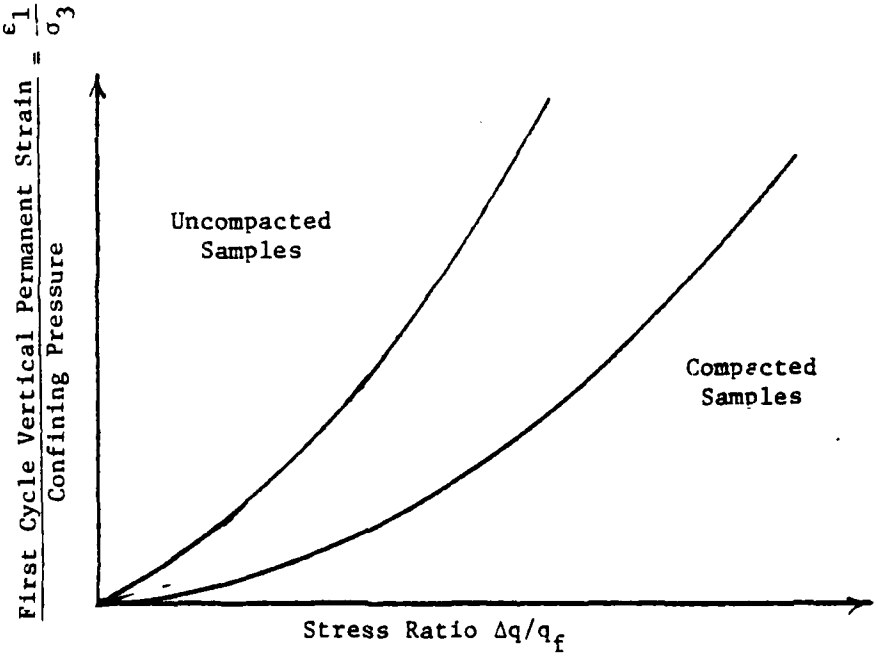

Figure 6. Selig's (1981) Laboratory Curves for Determining First Cycle Set Strain

is modified to provide an improved agreement between element stresses and strains. Between three and five iterations are usually sufficient to provide an accurate analysis using Hardin's model. The stiffness of the soil decreases with successive iterations.

Other relations established included a non-dimensional relationship for the unloading shear modulus, G_u, and the unloading shear strain, γ_u. For a silty sand and a silty clay soil the permanent set strain, S, was related to the number of load applications N, by

$$S = 1 + \log_{10} N \tag{4}$$

where γ/γ_r was less than 0.3.

Y. T. Chou and R. H. Labbetter (1973) reported on the behavior of flexible airport pavements underloads. He reported about theory and experiment. One purpose of their study was to reduce and analyze the deflection, stress and strain data obtained from a series of multiwheel aircraft flexible pavement tests. The second purpose was to establish relations between load and pavement response.

It was reported that, since pavement materials possess non-linear material characteristics, the use of non-linear finite element solutions seemed to be an obvious solution scheme. However, the development of the constitutive relations at that time could not adequately express the complex stress changes in a pavement system. Despite the nonlinearity of pavement materials, the relations between stress and displacements were linear in some aspects and the principal of superposition was reasonably valid.

Brown (1974) did some research into repeated loading testing of a granular material in a triaxial chamber. He established that, for a

dynamic deviator stress, q, equal to twice the mean value, p, both the resilient strains and permanent strains changed very little after 10^4 cycles. The permanent strain, ε_p, was linearly related to the applied stress by $\varepsilon_p = 0.01\ q/\sigma_3$, where σ_3 is confining pressure. The resilient strain, ε_r, was related to the applied stress by

$$\varepsilon_r = 237 \left\{\frac{q}{p+.25\sigma_3}\right\}^{1.54} \text{ microstrain} \qquad (5)$$

McLean and Brooker (1975) did a study to estimate the permanent deformations in asphaltic concrete due to repeated traffic loadings. In their article, they discussed a methodology to estimate permanent deformations (rutting) in pavements from repeated load triaxial compression tests and creep tests. Analytical calculations were made to predict rut development using the elastic layer program CHEV5L. A viscoelastic analysis of creep prediction was done using the VESYSII program.

In the laboratory program, repeated triaxial load tests were made on asphaltic bound materials over a range of temperatures. The technique for estimating rut depth involved fitting a curve through the results of the repeated load tests. A third order polynomial was evolved relating the plastic strains (corrected for volume change), ε_p, to the number of stress applications, N, by

$$\varepsilon_p = C_o + C_1 \log(N) + C_2(\log N)^2 + C_3(\log N)^3. \qquad (6)$$

C_1, C_2 and C_3 were experimental constants with mean values of 0.85, 0.013, and -0.14 respectively. C_0 was the logarithm of the permanent

strains after the initial load application, ϵ_1^p. ϵ_1^p was influenced by temperature, stress, and strain levels. The following relationship was developed to show the influence:

$$\epsilon_1^p = K(\sigma_d \cdot \epsilon_0)^n, \tag{7}$$

where σ_d is the difference in axial and radial stress in triaxial compression, ϵ_o is elastic strain, and K and n were experimental constants dependent of temperature. Axial creep compliance was established through tension tests at various temperatures. The creep compliance $\psi_\epsilon(t)$ as a function on temperature, t, was defined as:

$$\psi_\epsilon(t) = \frac{\epsilon_a(t)}{\sigma_d} \tag{8}$$

where $\epsilon_a(t)$ is the axial strain, and σ_d is defined above.

The analytical procedure used an elastic analysis of a two layer system, asphalt over subgrade. The wheel load was applied over a circular area. The strains in the pavement system were related to the triaxial tests by assuming $\sigma_d = \sigma_x - \sigma_h$, where σ_x is the vertical stress and σ_h is the horizontal stress. The permanent deflections, δ^p, were computed by dividing the pavement into a number of layers of thickness ΔZ_i. The permanent strains in each layer were computed using the methodology described above. The sum of the permanent deflections, $\epsilon_i^p \times \Delta Z_i$ of each layer were summed to yield the total surface deflections, or

$$\delta^p = \sum_{i=1}^{\text{No. of layers}} (\epsilon_i^p \cdot \Delta Z_i) \tag{9}$$

Poulsen (1978) reported on the laboratory testing of cohesive subgrades. Potential modes of distress for subgrates were considered to be directly or indirectly related to (1) elastic or resilient loadings caused by traffic loadings, (2) permanent or plastic deformations, and (3) plastic deformations caused by climatic or environmental changes, as changes in soil suction, freeze-thaw, or differential settlement. Poulsen directed his research to determining the relation between plastic deformations and traffic loadings.

His procedure was to take undisturbed samples from 6 countries including England, West Germany and the United States. The samples were subjected to triaxial repeated load tests. A constant confining pressure and a vertical static preload were applied to all samples. The minor principal stress ranged from 5 to 10 kPa (0.7-1.4 psi). The major principal stress was approximately twice the minor principal stress. A vertical dynamic stress, σ_{dyn}, was superimposed on the static stress state.

To establish a true picture of the process of permanent strain accumulations for a given σ_{dyn}, a large number of cyclic load tests were done. A basic simple expression

$$\varepsilon_p = e_1 N^{e_2} \beta^{e_3} \tag{10}$$

was presented to represent the test results. e_1, e_2, and e_3 were material constants. N was the number of load applications in a single stage test. β was the ratio $\sigma_{dyn}/\sigma_{dyn,f}$ called the degree of failure, where $\sigma_{dyn.f}$ was the dynamic deviator stress at triaxial failure for N - 100,000 cycles. The equation was considered valid for N greater than

100 cycles and β less than one. The proposed equation had no apparent correlation with general soil parameters.

Majidzadeh et al. (1978) reported on the rutting evaluation of subgrade soils in Ohio. The object of the report was to study rutting experimentally by using laboratory prepared samples subjected to uniaxial dynamic testing. The following rutting model was appropriate to the five types of silty soils used in the study:

$$-\varepsilon_p/N = A\, N^m \tag{11}$$

where ε_p is the permanent strain, N is the number of stress applications, m is the slope of the straight line relation between $\log(\varepsilon_p/N)$ and logN, A is ε_p at N equal to 1. The parameter m varies between 0.85 and .90.

The rutting parameter A was established as a function of E*, the dynamic modulus, by

$$A = R(E^*)^{-C} \exp\{\sigma_{apl}/\sigma_{ult}\}. \tag{12}$$

R and C are experimental constants. σ_{apl} is the applied stress and σ_{ult} is the ultimate stress from an unconfined strength test.

Frazier, Parker, et al. (1979) reported a structural design procedure for rigid airport pavements. They selected as a response model for the pavement system the computer code BISTRO. The code models the pavement as layered elastic materials. The design criteria was based on the tensile stress of concrete as computed by the program and the strength of concrete as measured by flexural beam tests. The limiting stress criteria was related to the number of coverages through fatigue

testing and converting the traffic load of multiple types of aircraft to an equivalent loading of a single aircraft.

They also reported in the Appendix the engineering behavior of pavement materials. They reported on many different materials in pavements and their general engineering behavior due to repeated loadings. A summary is given below.

The effects of repeated loadings for concrete were generally handled indirectly by fatigue relationships. However, the magnitude of stress sustained before cracking was a function of the number of repetitions, and the magnitude of this stress decreased as the number of repetitions increased.

Bituminous materials were reported to be viscous and temperature dependent. Their behavior was affected to a greater extent by the rate of loading than by chemical composition. Complete characterization requires different rates of loading so runways, taxiways and aprons could be adequately characterized. From a practical point of view, the rate of loading and temperature variations are limited. It is possible to include the effects of the loading rate and temperature variations during repeated load tests.

Granular bases were reported to be extremely difficult to characterize. The state of stress, particularly the confining pressure, was the dominating factor in determining the load deformation properties. Repeated load properties were different from static properties. Repeated loads tend to increase the stiffness, provided a progressive shear failure does not occur. Poisson's ratio, ν, was reported to vary during shear failure and the direction of change was dependent on the initial density. For low density soils, densification occurs during

shear, and ν decreased. Poisson's ratio would increase if the material increased in volume during failure. In general, ν reaches a relative constant value during repeated load tests and will remain constant unless shear failure occurs.

Subgrades were reported to be the components of a rigid pavement system most affected by repeated load applications. Most natural soils, when in the saturated condition, behave primarily like cohesive soils.

Snaith et al. (1980) reported on flexural pavement analysis. Their research was applied to vehicular pavements. They used the finite element program DEFPAV as a pavement model and were able to simulate creep behavior, crack propagation through the bitumunious layer, and compute the transient deflections with different cracking ratios. They also calculated the growth of rut depths and compared their calculations to a test section.

The creep characterization of the pavement materials was derived from repeated load triaxial tests. The creep equations for the subgrade soils used a non-iterative procedure to relate the induced permanent strain to the imposed stress. The surface deflections were computed by summing the displacements in the elements by

$$\delta = \sum_{i=1}^{\text{No. of elements}} \varepsilon_i h_i, \tag{13}$$

where ε_i was the element permanent strain and h_i was the height of the element. Their work was extended to overlay pavement design.

Selig, et al. (1981) developed a methodology for computing the cumulative permanent deformations of a railroad track structure due to traffic loading. They wanted to use this procedure as a basis for determining the maintenance life. They used a computer model called

GEOTRACK. Available information on the elastic and inelastic properties of ballast and subgrade materials was reviewed. Static and cyclic triaxial tests were carried out on granite ballast. Their methodology of computing permanent strain was compared to permanent strains on the FAST track.

They concluded that the vertical permanent strains after the first loading cycles could be predicted by two methods. One was to use the results of cyclic test results which depict the permanent strains as a function of the ratio $\Delta q/q_f$ where

$$\frac{\Delta q}{q_f} = \frac{\sigma_1-\sigma_3}{(\sigma_1-\sigma_3)f} = \frac{\sigma_1-\sigma_3}{\dfrac{2c\cos\phi + 2\sigma_3\sin\phi}{1-\sin\phi}} \tag{14}$$

σ_1 is the triaxial normal pressure, σ_3 is the confining pressure, c is the cohesion, ϕ is the angle of internal friction, and the subscript f refers to failure conditions. Typical lab curves are shown in Figure 6. The induced strain is a function of the soil properties c and ϕ, and the stress level.

The second procedure for computing the permanent strain after one cycle, ε_1, was to use hyperbolic parameters from static triaxial tests. The axial strain predicted by hyperbolic modeling, ε_v, can be computed from

$$\varepsilon_v = \frac{\sigma_1\,\sigma_3/E_i}{1-\dfrac{(\sigma_1-\sigma_3)\,R\,\,(1-\sin\phi)}{2c\cos\phi + 2\sigma_3\sin\phi}} \tag{15}$$

where R_f was defined as the failure ratio and E_i was the initial tangent modulus equal to $K\sigma_3^N$, where K and N were experimentally determined constants. The value of ε_1 can be computed by Equation 16 from ε_v if the resilient strain after the first cycle, ε_{r1}, is known.

$$\varepsilon_1 = \varepsilon_v - \varepsilon_{r1} \tag{16}$$

ε_{r1} has to be determined from testing and has shown to be related to $\Delta q/q_f$ as shown in Figure 7.

The value of the permanent strain after N cycles, ε_N, was related to the first cycle permanent strain by a laboratory analysis of cyclic triaxial testing. Both a linear and non-linear equation were presented for ballast.

$$\varepsilon_N = \begin{cases} \varepsilon_1 (1+ 19 \log_{10}(N1) & \text{linear equation} \quad (17a) \\ \varepsilon_1 (.85+.38 \log N+\varepsilon_1(.05)-.08 \log N) & \text{non-linear equation} \quad (17b) \end{cases}$$

A comparison of the computed strain values and actual strains in FAST track compared favorably.

Conclusion

A brief description of the methods of computing residual displacements and the knowledge of the behavior of pavement materials as developed over the past twenty years has been presented. The current method of computing residual displacements involves the use of finite element or elastic layer theory computer programs to compute the initial set strains due to the first loading. Final set strains are related to the initial set strains via actual testing of the material under triaxial conditions. The final rut depths are computed using Equation 2. These types of procedures are valid as long as the pavement materials do not undergo shear failure. Monograph solutions are also available but were not mentioned in the Literature Review.

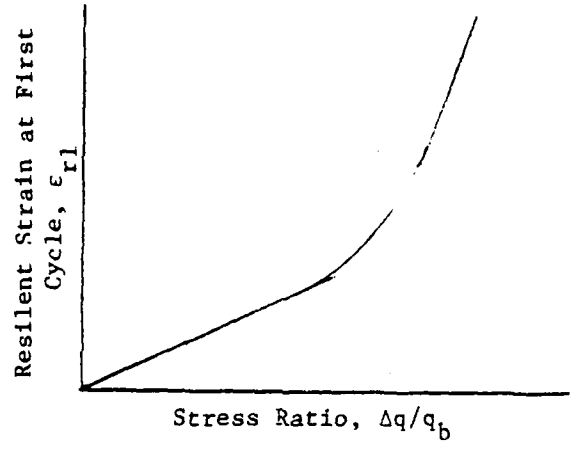

Figure 7. Selig's (1981) Laboratory Curve for Resilent Strain After One Cycle

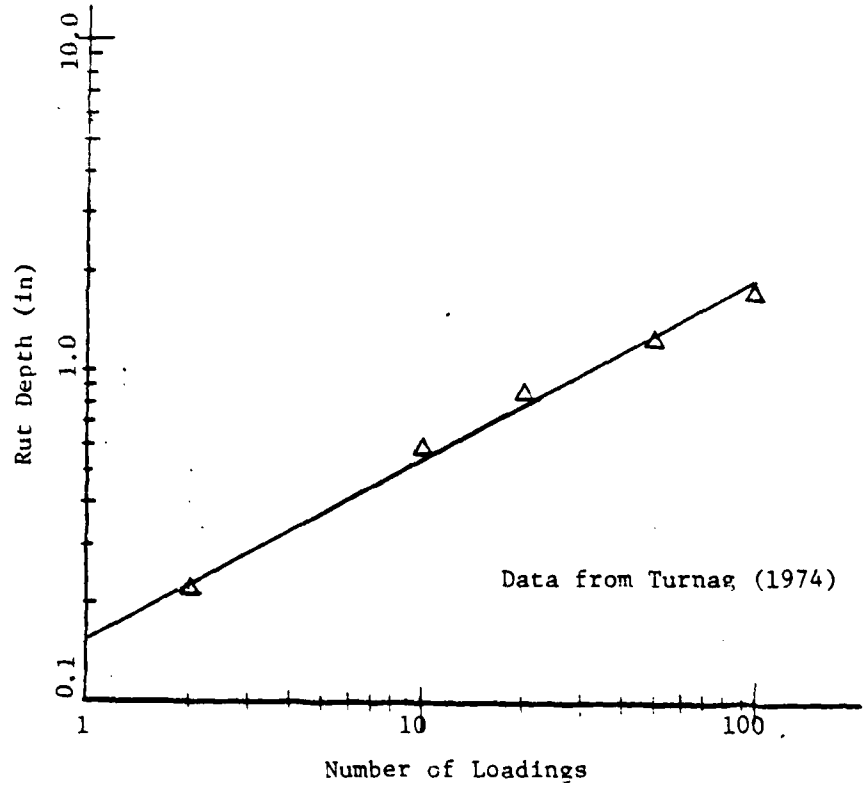

Figure 8. Rut Depth Versus Number of Load Applications of C-130 Tire on Buckshot Clay

CHAPTER III

Methodology for Computing Residual Displacements

Introduction

In this chapter two methodologies for computing residual displacements in surfaced and unsurfaced pavement systems are presented. All these methods involve the use of finite element computer codes. Trial solutions for two of the methods were attempted with varying degrees of success. To develop each procedure to a state where it could be used as an everyday tool was beyond the scope of this project. Sample solutions were attempted to determine the feasibility of each procedure rather than to fully develop an excellent software package for each method.

Procedure No. 1

The procedure discussed in this section closely approximates the state of art of residual displacement computation as revealed by the literature review. It has three basic steps. First, finite element computer codes were used to predict the permanent strains induced by one pass of an aircraft tire over a pavement section. Secondly, the vertical strains induced by repeat load applications was estimated by using laboratory triaxial repeat load data. Thirdly, the surface deflections were computed by summing the change of height of each element. Mathematically this was expressed by

$$S = \sum_{i=1}^{Num} \varepsilon_i * h_i \qquad (18)$$

where S is the surface deflection, ε_i is the element strain induced by repeated loads, h_i is the height of each element, and Num is the number of elements beneath the surface where the rut depth is being calculated.

Two different computer programs were used to compute the initial residual strains after one wheel load. These were the Bomb Damage Repair (BDR) code (Rude, 1980) and the Culvert Analysis and Design (CANDE) code (Katona, 1976). These codes were selected because they contained the non-linear material law developed by Hardin (1971).

The BDR code can represent pavement systems either with an axisymmetric mesh or with a mesh composed of prismatic solid elements. Only the axisymmetrical mesh was used. The CANDE program was developed to design and analyze buried culverts using two dimensional plane strain elements for soil and beam column elements for the culvert. Pavement systems were represented using the quadlateral elements and omitting the beam column elements.

The calculations using the BDR code were done at Tyndall Air Force Base during the summer of 1980. The program was written for CDC machines. A great deal of time was used to attempt to adopt the BDR code to the host IBM computer at Virginia Tech (VPI&SU). The program was not successfully running towards the close of the project, so much of the sample problems were done using CANDE. CANDE was the only other program known to contain Hardin's soil model.

According to the literature review, the greatest permanent strains occur during the initial application of the wheel load. Most pavement materials exhibit a non-linear relation between stress and strain. A non-linear stress-strain law seemed the most appropriate type of law to use to represent the initial load. Hardin's law was chosen to represent the pavement materials because of its non-linear nature and correlation to traditional material characterization parameters as void ratio density and plasticity index.

A typical stress strain curve for a non-linear material undergoing cyclic loading is shown in Figure 2. Shown in the figure are the initial tangent modulus E_i, the unloading modulus, E_u, the permanent strain after one cycle, ε_1, and the permanent strain after N cycles, S_N. The literature review has shown that S_N can be defined in terms of ε_1 by a logrithmic expression or a hyperbolic power expression.

For the equation S_N to be used to compute the permanent set strain, the initial set strain ε_1 must be determined. Using a finite element computer, this would involve loading the mesh using a variable modulus and then removing the effects of the load using the unload modulus. None of the available computer codes contained the programming to apply and successfully remove a load.

The following method was adopted to compute ε_1 instead. The aircraft wheel load was applied to the pavement using non-linear constitutive material models. This analysis corresponds to the loading phase. To approximate the unloading phase, the same wheel loading was applied to the same grid, but all materials were represented by the initial tangent modulus. The initial tangent modulus was assumed to be equal to the unload modulus. In reality this is only approximately correct. The element strains in the unloading phase were subtracted from the element strains obtained during the loading phase to yield the permanent set strains after one cycle.

Several attempts were made to simulate unloading by using two loading increments with the CANDE program with little success. The load was applied during the first loading increment and a load of the same magnitude, but opposite sign, was applied during the second loading increment to zero out the first load. Unrealistic strains and

displacements were obtained. Hardin's lawwas used for these calculations. The CANDE program reduced the stiffness of any material when tensile stresses were applied. This stiffness reduction produced the unrealistic results. This is why only compressive forces were applied when using CANDE.

Other limitations were also discovered using the CANDE program to compute the first cycle residual strain in clay soils. Hardin's law is programmed to perform one to five iterations to find the appropriate secant shear modulus for a particular state of stress. The first cycle corresponds to using the maximum shear modulus. An analysis of "load" and "unload" calculations showed that the strains for the "unload" case were greater than the "load" case. This seemed theoretically impossible, so fine grain soils were modeled as linear materials. For the unload case, an initial tangent Young's modulus was used, and for the load case an appropriate secant Young's modulus was used.

Comparison of Procedure with "Buckshot Clays" Tests

G. W. Turnage, et al. (1974) perform large scale laboratory tests to correlate the ruts produced from two different types of aircraft tires and three standard military trucks. These tests were done on the "Buckshot clay" at various compacted densities that were placed in indoor, concrete-lined pits 6 feet deep and 11.7 feet wide by 13 feet long. A high strength clay was placed within 24 inches of the top of the pit and enough soil was compacted at specified densities and moisture contents using a 40,000 lb self-propelled, multiwheel roller to fill the rest of the tank.

The buckshot clay is a Mississippi River alluvium. It is a highly plastic, almost purely cohesive soil. It has a CH Unified Soil Classification. For the comparison study, test data with the soil compacted at a dry density of 104.2 pcf, at 22.5 percent moisture content, and a degree of saturation of 98.6 percent was used. The soil was trafficked with a C130 aircraft tire (20-20, 22 pr) with a total load of approximately 35384 lbs and a tire pressure of 100 psi. The aircraft tire was mounted on a carriage that spanned the tank. The carriage restricted the tire loading to a single path through the soil. An average force of 1549 lbs was used to tow the tire through the soil. The results of the rut depth versus number of repetitions is shown in Figure 8. The slope of a curve fitted through Turnage's data is 0.546.

For the computer modeling, the initial loading and unloading of the tire were simulated by applying a 100 psi pressure to the surface of the finite element grid shown in Figure 9. The CANDE program was used and the soil was modeled as a linear elastic material with a Young's modulus of E_L = 5700 psi for loading and E_u = 11400 psi for unloading. Poisson's ratio of the soil was 0.43. The computed permanent strains after one cycle were obtained by subtracting the respective element strains computed using E_u from the element strains computed using E_L. The total rut depth was computed using Equation 18.

Turnage's report did not contain repeated load test data on the "Buckshot Clay". They were obtained by assuming an empirical relation between accumulated strains and the initial permanent strains. The assumption was made that the permanent strains would accumulate as the same rate as the total rut depth. Using the data provided in Figure 8 and the mathematical formulation suggested by Poulsen, the following

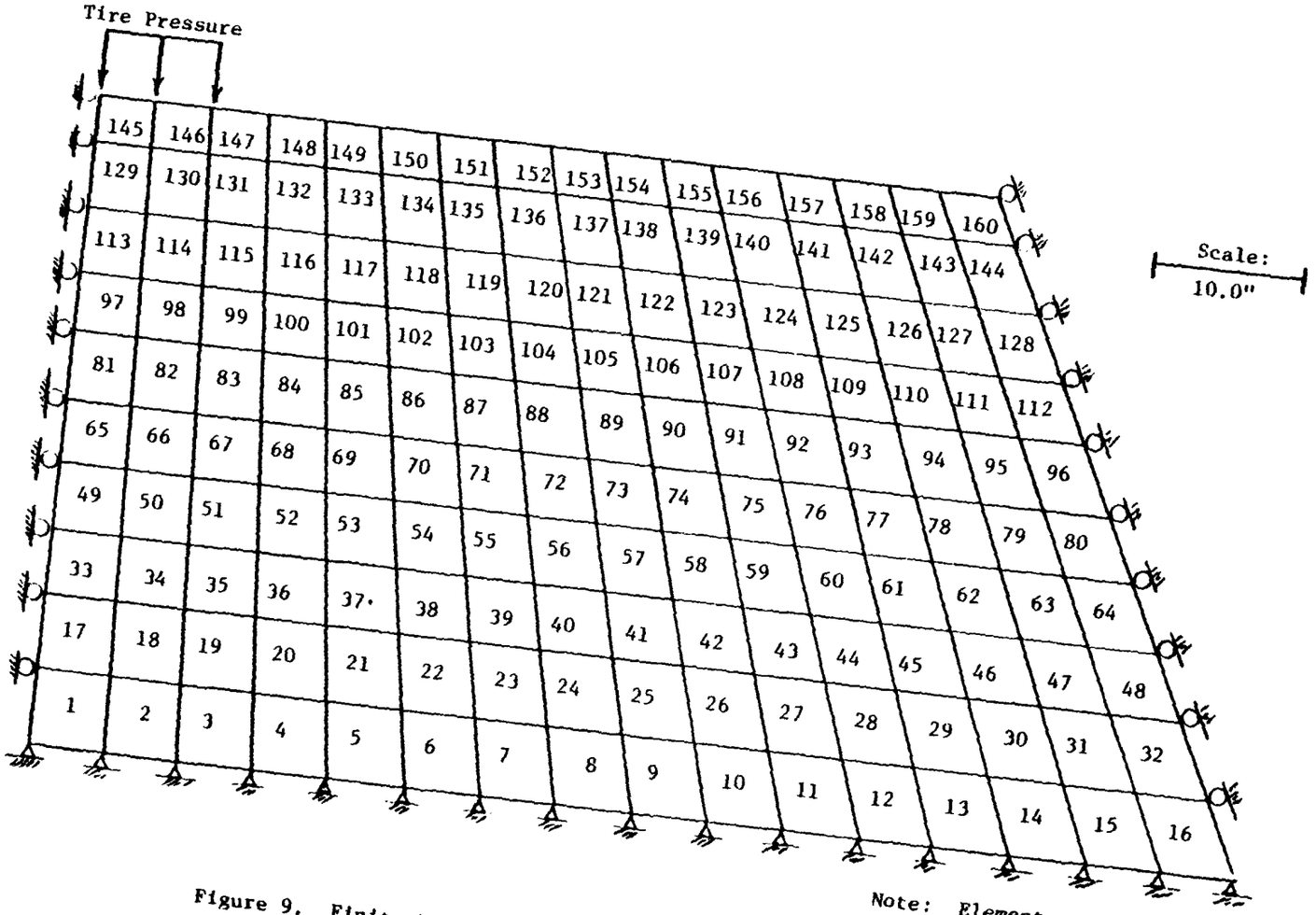

Figure 9. Finite Element Grid Used by CANDE Program

Note: Element numbers are shown

expression was obtained: $\varepsilon_p = \varepsilon_1 N^B$, where B = 0.546, N = number of load applications, ε_1 = permanent strains after one cycle and ε_p = accumulated set strain.

Table 1 summarizes the calculations for the finite elements beneath the center of the wheel pressure. The initial rut depth of 0.14 in agree with the extrapolated test value of 0.155 in. The final rut depth of 1.73 in agree well with the actual value of 1.77 in after 100 passes.

Additional data from Turnage's tests were plotted in a graph of rut depth versus number of applications. The test results corresponded to the application of a C-130 tire with the "Buckshot Clay" compared at different densities at different moisture contents. See Figure 10. The slopes of each curve are approximately equal.

Turnage also reported the results of a cone penetrometer test for each filling of the testing tank. Figure 10 also shows the results of plotting the rut depth after the first pass versus the cone index. The cone index, CI, was the force (in lbs) per unit area of the cone base required to penetrate the soil in a vertical direction at a rate of 72 in/min. The cone was a right angle cone with a 30° apex angle and a 0.5 in^2 base area. These results would tend to indicate that a cone penetrometer test could be used to estimate the first rut depth, h_i, and the expression $h = h_1 N^{\beta}$ could be used to estimate the rut depth, h, produced after N loadings. If the hypothesis is carried further, the same relations could hold for estimating rut predictions via computer analysis.

Table 1

Summary of Calculations for Permanent Rut Depths in "Buckshot Clay"

Element Number	Element Height h (in)	Unloading Strain, ϵ_u (in/in)x10^{-3} Using E_u = 11400 psi	Loading Strain, ϵ_L (in/in)x10^{-3} Using E_L = 5700 psi	First Cycle Set Strain, $\epsilon_1 = \epsilon_L - \epsilon_u$ (in/in)x10^{-3}	Element Deformation after 1 cycle $\epsilon_1 h$ in x 10^{-2}	Set Strain After 100 cycles, ϵ_{100} (in/in)x10^{-3} $\epsilon_{100}=\epsilon_1(100^{.546}$	Element Deformation After 100 Cycles, $\epsilon_{100}h$ (in x 10^{-2})
145	3.6	- .39	- 7.8	-7.41	-2.7	-9.16	-3.29
129	4.4	-5.10	-10.0	-4.9	-2.2	-6.06	-2.66
113	3.8	-4.6	-9.2	-4.6	-1.7	-5.68	-2.16
97	3.7	-3.9	-7.9	-4.1	-1.5	-4.94	-1.33
81	4.5	-3.4	-6.7	-3.3	-1.5	-4.08	-1.83
65	4.5	-2.8	-5.7	-2.9	-1.3	-3.58	-1.61
49	4.3	-2.4	-4.9	-2.5	-1.0	-3.09	-1.30
33	4.2	-2.1	-4.2	-2.1	-0.88	-2.59	-1.30
17	5.0	-1.7	-3.4	-1.7	-0.86	-2.10	-1.05
1	5.0	-1.2	-2.5	-1.3	-0.61	-1.60	-0.80

$\Sigma\epsilon_1 h$ = -0.142 in. $\Sigma\epsilon_{100} h$ = 1.733 in.

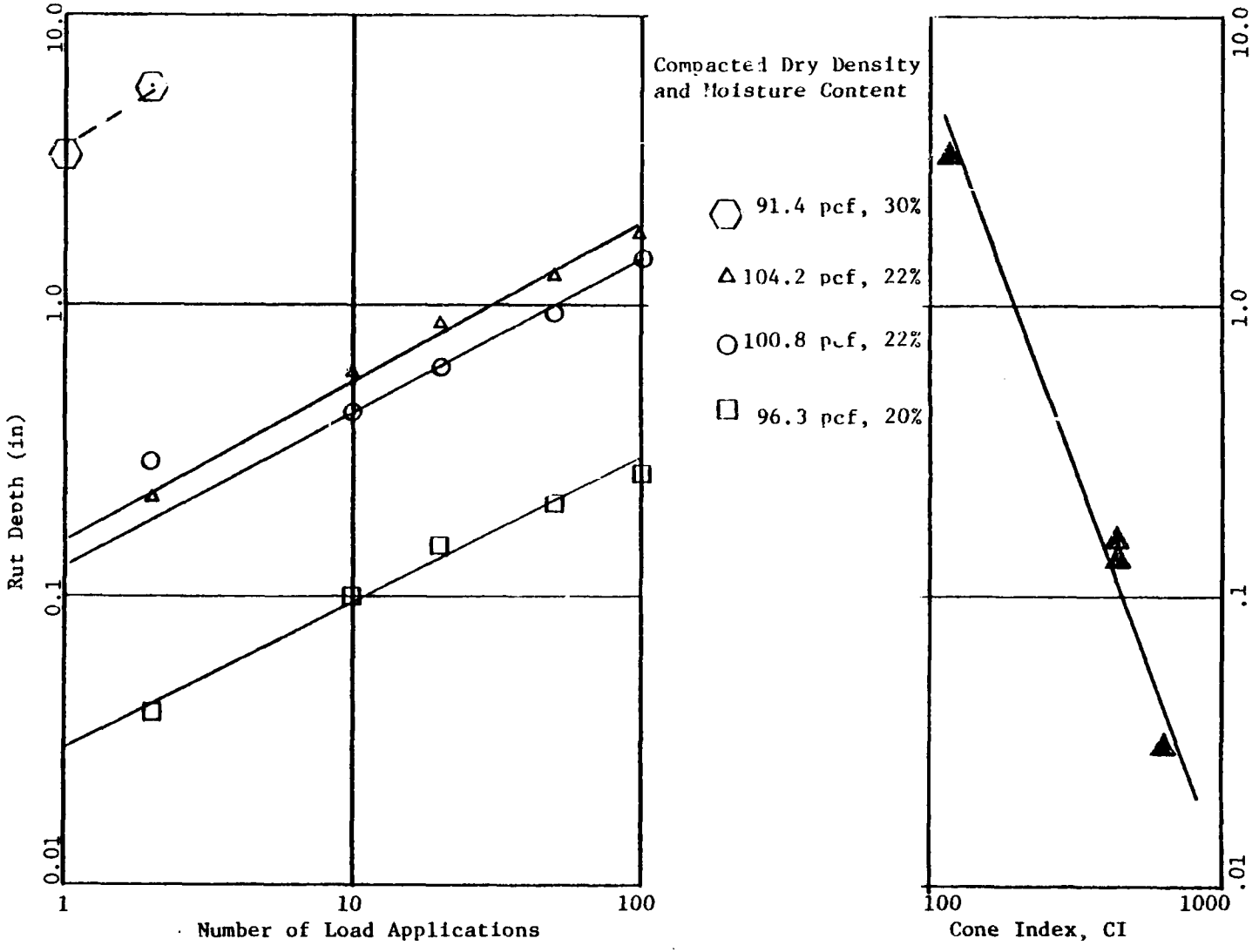

(a) Rut Depth Versus Number of Load Applications for a C130 Tire

(b) Initial Rut Depth Versus Cone Index for a C130 Tire

Figure 10. Graphic Presentation of Turnage's (1974) Data

Evaluation of Crushed Limestone Crater Repair

The current method for an expedient repair of a runway crater involves four steps. These are: (1) pushing debris into the crater up to 24 inches below the pavement surface, (2) placing select fill (crushed limestone) into the crater and overfilling by approximately 6 inches, (3) compaction using a self propelled vibratory roller and (4) placement of a Foreign Object Damage (FOD) cover. The Engineering and Services Laboratory at Tyndall Air Force Base, Florida have conducted several simulated repairs and have trafficked them with an F-4 load cart. One repair was briefly reported by Rude (1980) and three were reported in detail by Knox (1980).

The repair reported by Rude (1980) was made by placing 24 in of crushed limestone into a simulated crater. At the bottom of the crater was a clay soil. The repair was trafficked by 1440 coverage of an F-4 load cart distributed among twelve paths. The maximum number of passes on any strip was 150 passes of the load cart. Figure 11 shows a simulated picture of the crater profile after 1440 coverages. The profile was obtained by subtracting the elevation at selected points in the repair after trafficking from the elevation before trafficking. The repair was assumed to be level after the compaction process was completed. The average rut depth for the area that received 150 passes was 1.87 in.

Rude (1980) used the Bomb Damage Repair (BDR) Computer Program to estimate the ruts produced by an F-4 wheel loading. THe BDR program used Hardin's law to represent the stress-strain behavior of both materials. Using the procedure discussed in the theory section, the permanent strains after one pass of an F-4 load cart as calculated from

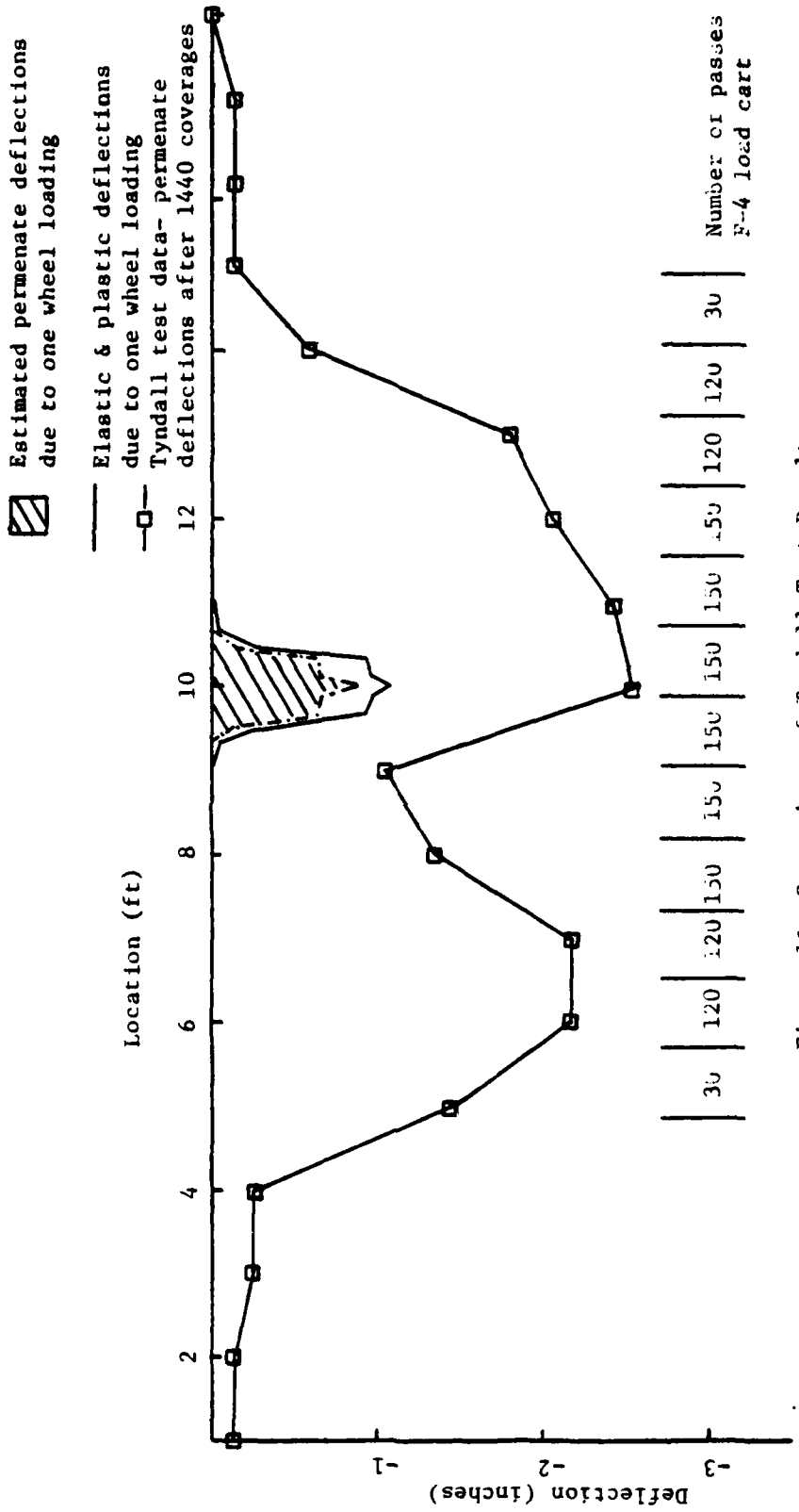

Figure 11 Comparisom of Tyndall Test Results and B.D.R. Code Results for Surface Deflections

the BDR calculations was 1.12 in. The relationship that the accumulated set strains $\varepsilon_N = \varepsilon_1(1+.19 \log N)$, where ε_1 = first cycle set strains and N = number of load applications, was used to predict the rut depth after 150 passes. The calculated rut depth was 1.61 in. This prediction was 13.5% of the average value. Only the strains in the finite elements within the top 12 in. of the select fill and the top 10 in. of the clay had any significant contribution to the rut development. Significant element strains produced a permanent settlement of 0.001 in. or greater.

The crater repairs reported by Knox (1980) were conducted for the purpose of field testing the rapid repair technique and to evaluate the repairs with a F-4 load cart. Three crater repairs were properly made using crushed limestone placed on debris backfill. Crater repair number three had an average of 2 1/2 ft of crushed limestone, crater repair number five had approximately 36 in. of select fill, and crater number six had between 18 in. to 30 in. of select fill. Each repair received 1440 coverages of an F-4 load cart. Crater 3 was repaired after 100 coverages by additional amounts of limestone due to consolidation of the repair. Repairs number five and six received 96 coverages of the F-4 load cart immediately after being made. An additional 1344 coverages were made during the next 16 days. The delay was due to repairs required to the F-4 load cart. The maximum rut depth due to repairs three, five and six were 1.7 in., 0.8 in., and 1.4 in., respectively. Knox reported that the time delay in trafficking the repairs probably resulted in the abnormally small surface deflections for repairs five and six.

The CANDE computer program was used to simulate crater number six. The depth of the select fill was assumed to be 24 inches. The computer

program was used to calcualte the element strains due to applying the F-4 wheel load and removing the load. The difference in these strains was the permanent strains induced after the first cycle. Hardin's soil model was used to represent the gravel. Five iterations were used for the loading and one iternation was used for the unloading. This push-back was modeled as a linear material.

Knox did not report field or laboratory information with regard to the "compacted" pushback material. Green (1978) summarizes elastic constants for airport material. Green reports on work by Foster and Heukelom that says the subgrade modulus for soil can vary from 1130 psi for peats to 127,000 psi for moraine deposits. No information was listed regarding the physical properties of pushback compacted according to the BDR repair procedure. Without actual values for the pushback material only ball-park estimates of rutting behavior were determined.

A wide range of values for the elastic modulus was chosen to represent the behavior of the pushback material. The results of the series of calculations are shown in Figure 12. Plotted on the vertical axis are the maximum surface vertical deflections (in inches) and plotted on the horizontal axis is Young's modulus of the pushback (psi) on a log scale. The upper curve represents the surface deflections for the loading case and the lower curve represents the unloading case. To compute the initial residual displacement after one cycle, the surface displacements according to curve B were subtracted from the surface displacement of curve A. These results agreed well when equation 18 was used to compute the first cycle permanent deflections.

Data analysis indicates that in the limiting case where the modulus of the pushback is exceptionally high, the select fill deflects 1.30 in.

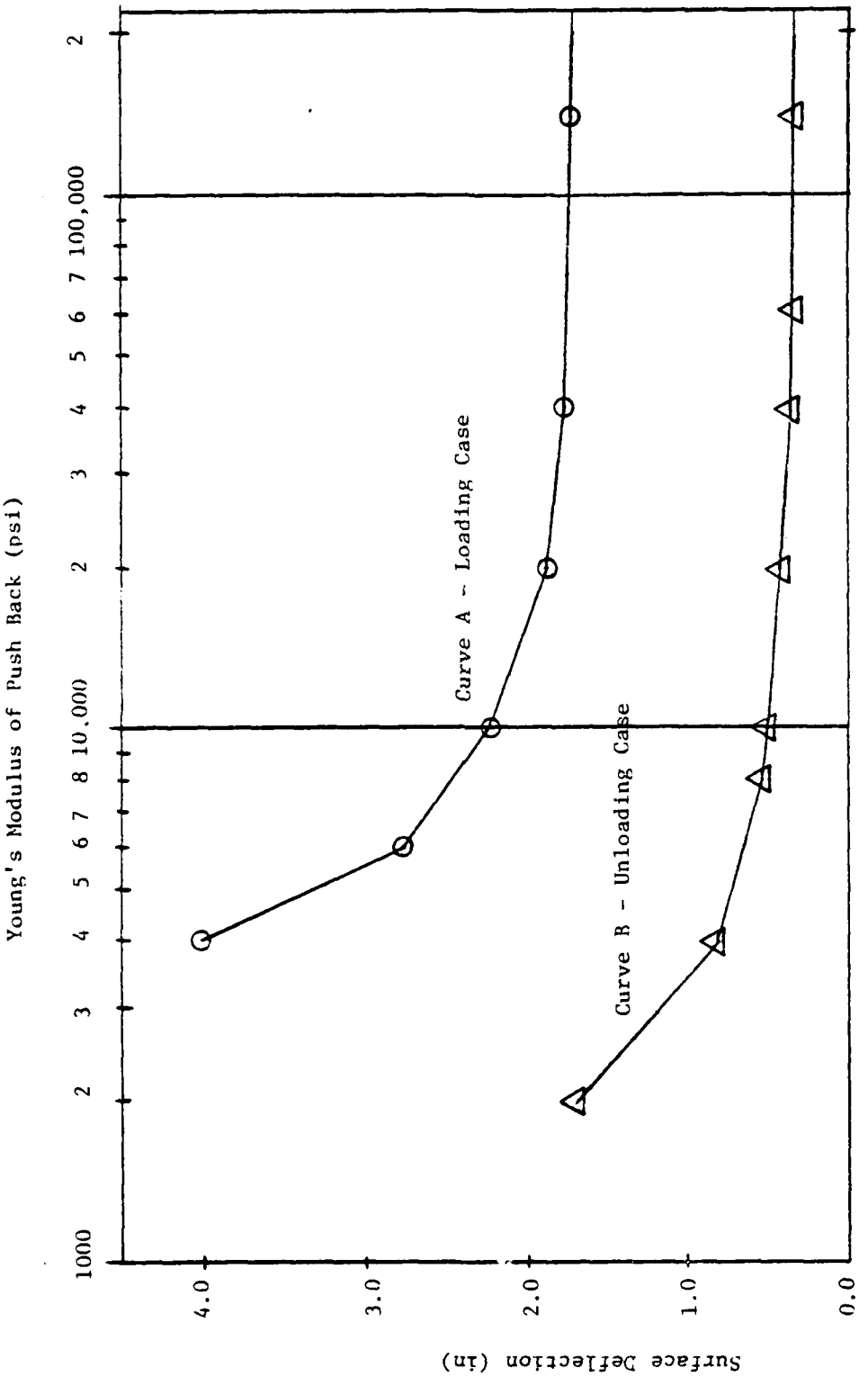

Figure 12. Effects of Varying Modulus of Pushback Material on Surface Deflections of an Expedient Crater Repair

after one loading, and has a permanent rut deflection of 1.85 inches after 150 passes. If the pushback was highly compacted with an unload modulus of 60,000 and a load modulus of 6,000 psi, the first cycle permanent deflection of the repair would be 2.37 in. and the maximum rut depth after 150 cycles would be 3.72 in. In this estimate, the select fill was assumed to behave according to the relationship $\varepsilon_p = \varepsilon_{p1}(1+.19 \log N)$ and the pushback according to the relationship $\varepsilon_p = \varepsilon_{p1}(1+\log N)$ where ε_{p1} is the residual element strain after one cycle and ε_p is the residual strain after N cycles. The permanent surface delections were computed accroding to equation 18.

The computed results were much larger than reported by Knox. The average depth of the select fill could have been less than the 24 in. assumed. The plane strain elements in the CANDE program may not be applicable for this crater repair. Improved calculations might result if a finer finite element mesh has been used. In general, however, an estimated range of deflections from 1.3 in. to 3.72 in. does not seem to be unreasonable.

A possible field check to determine proper compaction of pushback material would be to employ a cone penetrometer. Sanglerat (1972) has reported a number of research projects where correlations have been established and confirmed by other researchers for compaction control using the one penetrometer. Computer analysis of a particular repair plan could determine limiting values for subgrade modulus and densities for the pushback. Correlations could be established between different densities of pushback and cone penetration values. The cone penetrometer could then be used as a field check to determine if sufficient compaction had been achieved.

Applications to Airport Pavement

A sample problem was generated to apply the method for computing residual displacements to a concrete runway. The pavement section consisted of a concrete over a granular base with a stiff clay as a subbase. The properties and the height of each layer as idealized in the finite element grid are given in Table 2.

A series of calculations were made to determine the maximum rut depth under an F-4 wheel loading. The process previously described was used. The results of these calculations are shown in Figure 13. The horizontal axis is the number of repetitions, and the vertical axis is the maximum rut depth. The concrete was assumed to settle along with the pavement base and subgrade. The rate of induced strain due to load repetitions for each material is shown in Table 3.

In an actual runway, aircraft do not land or take off along a definite path. According to HoSang (1978), the aircraft traffic distribution can be represented by a theoretial normal distribution. The mean value is slightly offset from the centerline. A typical histogram for the lateral distributions of aircraft traffic during takeoffs is shown in Figure 14.

To illustrate the process of computing the residual displacements, a series of F-4 wheel loadings for a given number of total applications were distributed across the pavement section according to the distribution shown in Figure 14. The accumulated deflections were then calculated for the prescribed number of load applications. The total residual displacements for a total of 200, 20,000, and 200,000 load applications are presented in Table 4 and illustrated in Figure 15.

Table 2

Characteristic of Materials in CANDE Analysis of a Concrete Airport Pavement

Layer	Composition	Thickness (in)	Constitutive Law	Density (pcf)	Comments
1	Concrete	11.8	Linear Elastic $E = 3.0 \times 10^7$ psi $\nu = 0.3$	150	Rests on gravel
2	Gravel	12.7	Hardin Default	146	Void ratio = 0.18
3	Clay	18.5	Linear Elastic $E_L = 5700$ psi for loading $E_u = 11400$ psi for unloading	128	Similar to "Buckshot Clay"

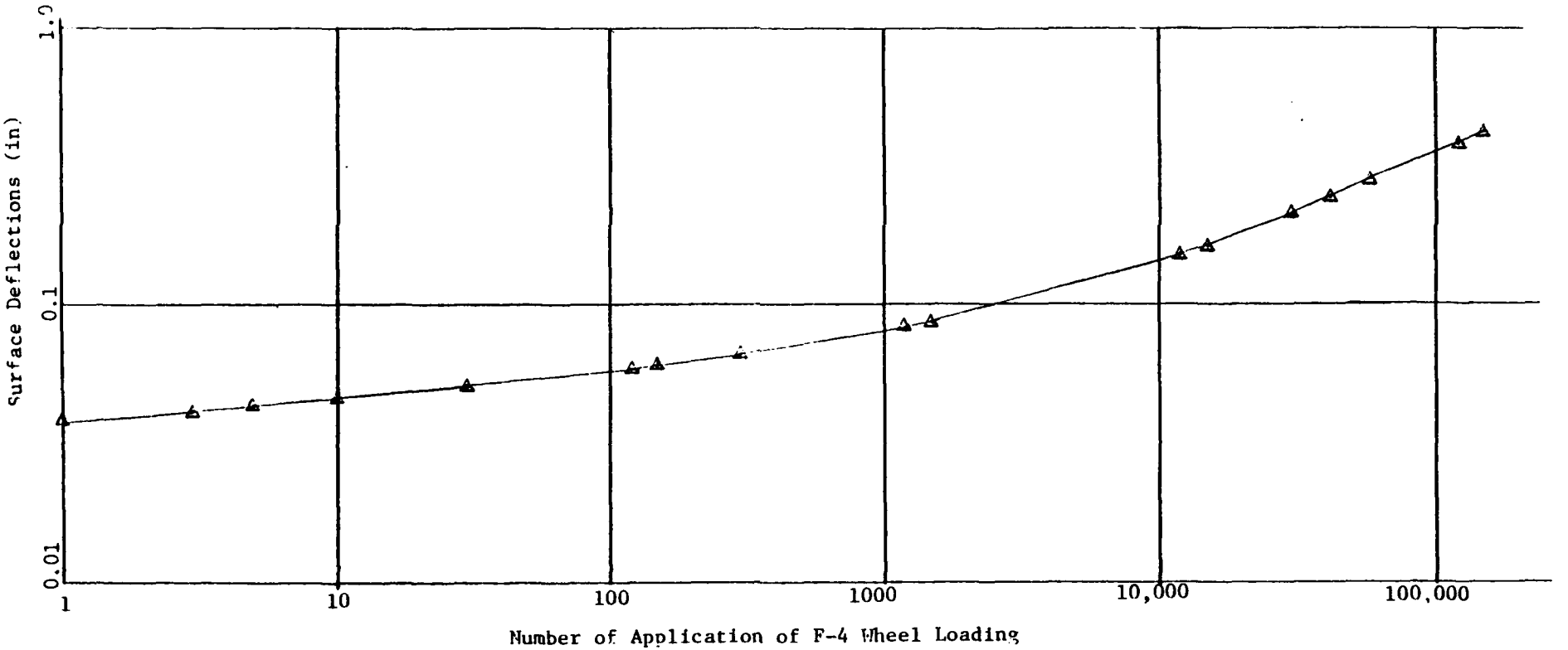

Figure 13. Surface Deflections of a Concrete Runway Section Due to Repeated F-4 Wheel Loading

Table 3

Rate of Induced Strain Due to Load Repetitions

Layer	Composition	Strain Accumulation Equation
1	Concrete	None
2	Gravel	$\varepsilon_n = \varepsilon_1 (1 + .19 \log N)$
3	Clay	$\varepsilon_n = \varepsilon_1 N^{0.55}$

N = number of load applications

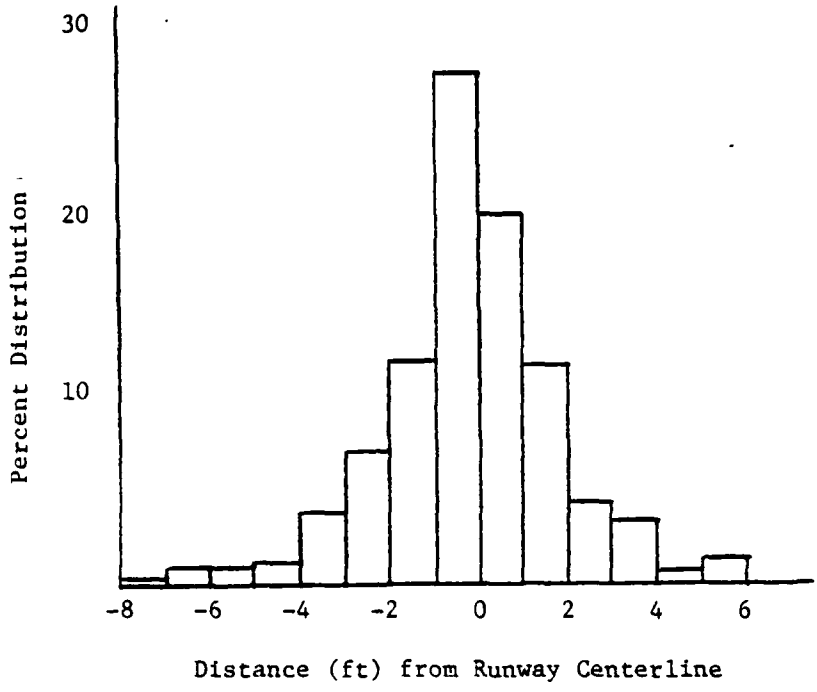

Figure 14. Typical Histogram for Lateral Distribution of Aircraft Traffic During Takeoffs, after HoSang (1978)

Table 4

Accumulated F-4 Wheel Loading Distributed Across Concrete Runway (in) x 10^{-2}

% Distribution	.05	1.2	1.2	1.3	4.2	7.5	12.5	28.5	20.6	12.3	4.6	3.5	0.75	1.3
2,000 Loadings	3.8	5.0	5.0	5.1	5.7	6.1	6.6	7.6	7.1	6.5	5.7	5.6	4.8	5.1
20,000 Loadings	4.6	6.6	6.6	6.7	8.2	8.9	10.0	12.8	11.6	10.0	8.0	7.8	6.1	6.6
200,000 Loadings	5.8	10.0	10.0	10.0	14.0	16.5	20.0	29.0	25.0	20.0	14.5	13.2	8.9	10.0

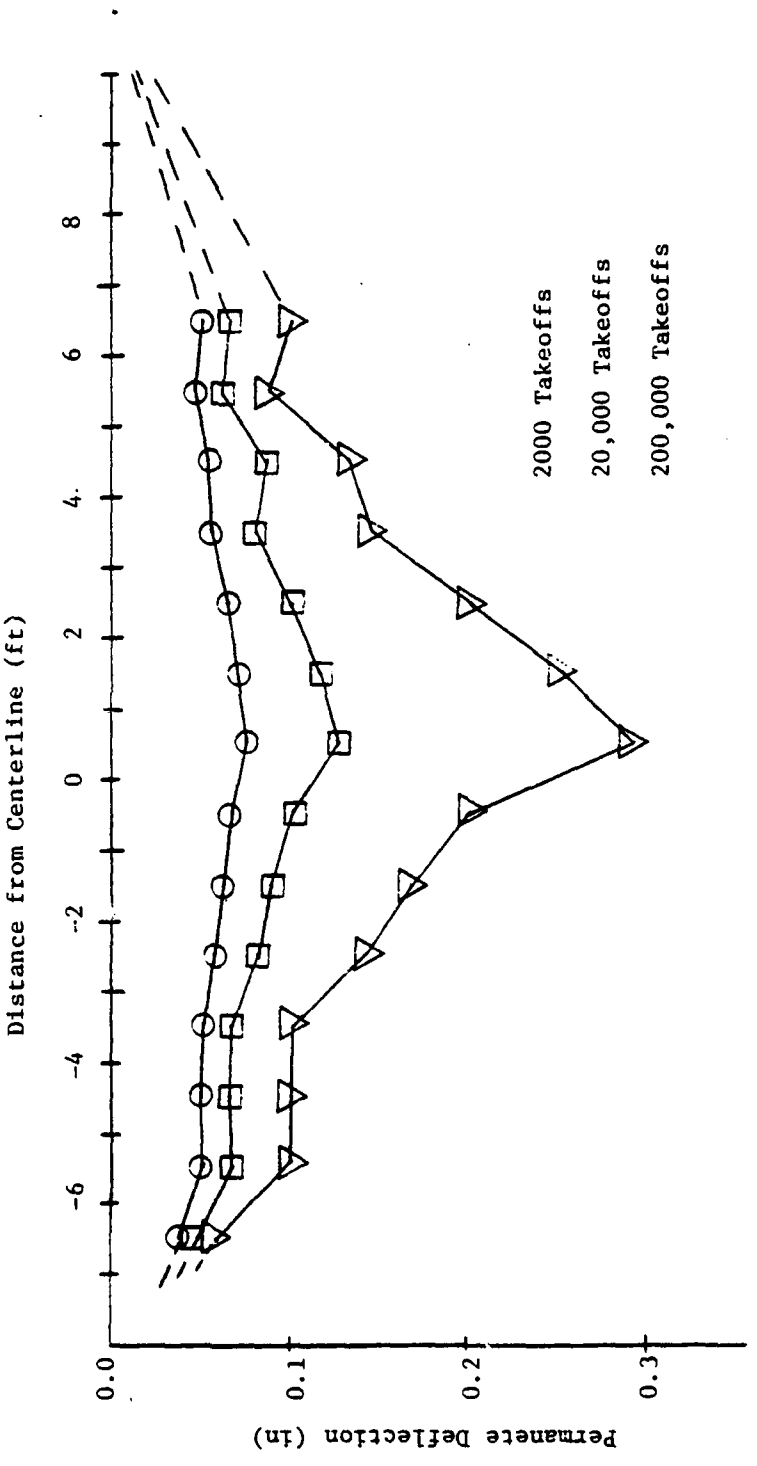

Figure 15. Permanete Deflections Across Concrete Runway

The illustrative example is very simplistic in that it represents that of only the application of one wheel loading and not the total wheel loading of an F-4 aircraft with its own landing gear configuration. An algorithm could easily be written to distribute the actual number of wheel loadings to a particular location on the pavement. If a particular airport is serving a mixed type of aircraft traffic, all landings could possibly be converted into an equivalent aircraft. One of the major assumptions of the analysis procedure was that only the permanent deflections made directly under the wheel were considered. With further refinement of the procedure, the permanent deflections away from the wheel could be accounted for.

Procedure No. 2

The second solution procedure involved the initial strain concept commonly used in the finite element method. A brief description of the initial strain concept is presented below. The procedure for computing residual strains using initial strains is then presented.

According to Desai and Abel (1972), initial strains in structural systems may occur due to a number of various influences as change in temperatures, creep, shrinkage, crystal growth and local insitu temperature changes. If $\{\varepsilon_o\}$ is a vector containing the initial strains and $\{\varepsilon\}$ is a vector containing the total strains, the vector $\{\varepsilon_e\}$ called the effective elastic strain vector can be defined by

$$\{\varepsilon_e\} = \{\varepsilon\} - \{\varepsilon_o\} \tag{19}$$

For elastic stress strain relationships

$$\{\sigma\} = [c]\{\varepsilon_e\} = [c]\{\{\varepsilon\} - \{\varepsilon_o\}\} \tag{20}$$

where $\{\sigma\}$ is the stress vector and [c] contains the material elastic constants that relate stress and strain. The strain energy function can then be written as

$$U = \frac{1}{2}\iiint_V \{\varepsilon\}^T(c)\{\varepsilon\}dv - \iiint_V \{\varepsilon\}^T(c)\{\varepsilon_o\}dv + \frac{1}{2}\iiint_V \{\varepsilon_o\}^T(c)\{\varepsilon_o\}dv \tag{21}$$

The net effect on equilibrium from the initial strains is an additional load term $\{Q_o\}$which represent the contributions of the initial strains.

$$[K]\{q\} = \{Q\} + \{Q_o\} \tag{22}$$

where $$\{Q_o\} = \iiint_V [B]^T[c]\{\varepsilon_o\}dv$$

[k] is the element stiffness matrix, $\{q\}$ is the nodal displacement vector, $\{Q\}$ is a load vector, and [B] is a matrix that relates strains and displacements. By using the additional load vector $\{Q_o\}$, the effects of the initial strains can be included in the finite element formulation. The initial strain procedure above was termed using elastic material laws.

For materials that behave in an elastic plastic fashion, the method described below uses the same stiffness throughout and thus shortens computational time. See Figure 16. Under the effects of load $\{Q\}$ and elastic stiffness [k], the solved displacement will correspond to point A. The correct equilibrium state would correspond to point B on the non-linear curve. The difference between the correct displacement $\{q_b\}$ and the computed displacement $\{q_a\}$ is $\{q_o\}$. The "initial strain",

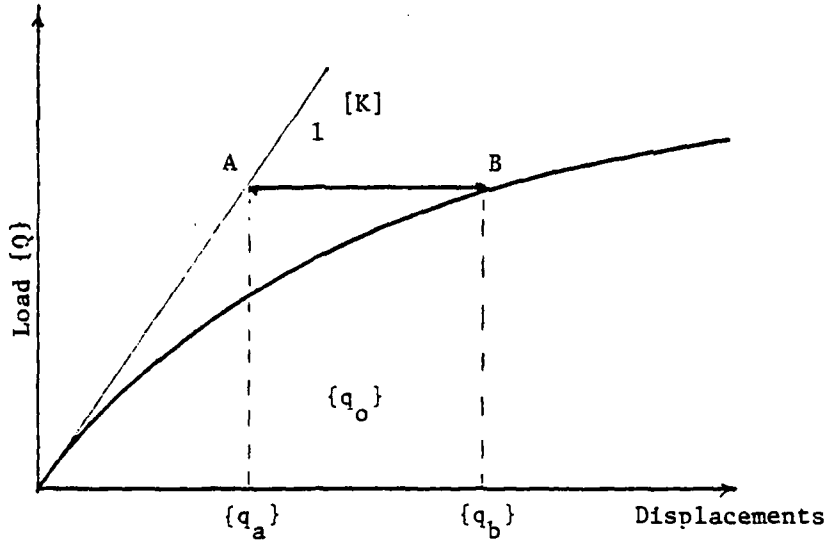

Figure 16. Initial Strains (after Desca and Abel (1972))

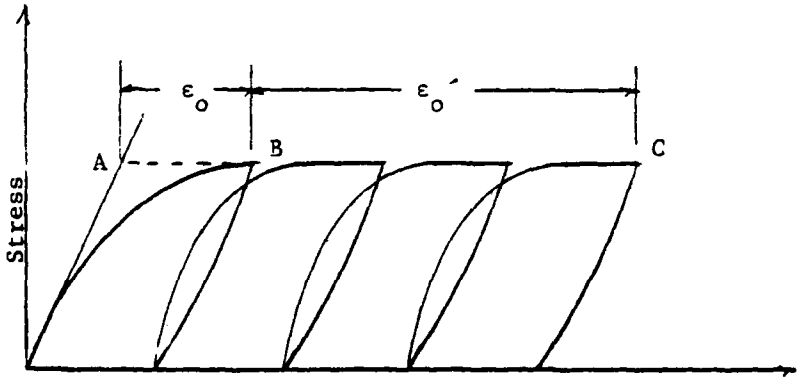

Figure 17. Initial Strain Procedure for Repeated Loadings of Non-Linear Materials

$\{\varepsilon_o\}$ corresponding to $\{q_o\}$ is $\{\varepsilon_o\} = [B]\{q_o\}$. The correction load is found by using

$$\{Q_o\} = \iiint_V [B][c]\{\varepsilon_o\}dv \tag{23}$$

The load is applied to correct the displacements from A to B.

Figure 17 represents a hypothetical stress strain for a non-linear material subjected to repeated loading. The initial strain procedure described above could be used to adjust the initial loading to point B. The strain state after repeated loading would correspond to ε_c and the "initial strains" would be $\varepsilon_o = \varepsilon_c - \varepsilon_B$. The corresponding correction load would be

$$\{Q_o\} = \iiint_V [B][c]\{\{\varepsilon\}_c - \{\varepsilon_B\}dv \tag{24}$$

To find the permanent set, S, the load would be removed using the unloading modulus.

An initial attempt was made to employ the initial strain procedure for computing residual displacements. In applying the procedure, tensile strains were generated in certain elements. If the corresponding tensile stresses exceed the tensile strength of the material, these stresses could be removed by reapplying the initial strain procedure or by eliminating the element from the global stiffness matrix and redistributing the load.

The development of a complete software to correctly perform this analysis was deemed beyond the scope of this feasibility study.

Conclusions

In this chapter, two methodologies for computing residual displacements in surfaced and unsurfaced pavement systems were presented. The

first procedure was by far the simplest and easiest to implement. The procedure requires the use of a finite element computer program and requires five steps:

(1) Computing element strains due to the appropriate wheel loading by finite element program.

(2) Computing element strains due to unloading conditions by finite element program.

(3) Computing the permanete set strains after one loading, ε_1, for each element by subtracting (2) from (1).

(4) Computing the permanete set strains for N loadings based on equations developed from laboratory triaxial testing.

(5) Computing surface deflections by summing the change of height of each element.

$$S = \sum_{i=1}^{\text{No. of Elements}} (\varepsilon_i * h_i)$$

Example calculations were worked using the first procedure. The first two cases consisted of computing residual displacement for aircraft tires on clay and an expedient crater repair. The sample calculations compare favorably with published data on the actual behavior. The third example considers a possible application to a concrete pavement and takes into account the fact that aircraft traffic is distributed across the runway's cross section.

The second procedure involves the application of the initial strain concept in finite element method of analysis. The initial strain concept would be used to formulate corrective nodal loads that would be applied to produce permanete displacements. The procedure was not

easily employed in that initial attempts to implement it produced tensile strains in the pavement materials. These tensile strains would not actually exist and would have to be eliminated from the finite elements before the corrective forces could be applied.

CHAPTER 4

Summary and Recommendations

Summary

Based on the literature survey and the sample calculations in Chapter 3, the computations of residual displacements are very feasible. Two different methodologies were proposed. The method that was the easiest to implement requires a finite element computer code and the results of laboratory repeated load tests on pavement materials.

Finite element programs were used to obtain the residual displacements after one load application. The use of non-linear material behavioral laws or were recommended. Relationships between the first cycle set strain and the set strain after N cycles were obtained from the triaxial test results. These relationship produced the final set strain for each element, ε_i. The surface deflections were computed by summing the settlements of each element or

$$S = \Sigma \varepsilon_i h_i \tag{25}$$

where S was the surface settlement and h_i was the height of each element. Sample calculations were presented to show the effectiveness of the procedure.

Recommendations

The recommendations for further research and development are listed below:

(1) Develop computer software to implement the proposed procedures.

(2) Conduct extensive laboratory repeated load tests on a wide variety of soils and pavement materials and derive general repeated load

characteristics that would be related to fundamental properties as density, void ratio, unconfined compressive strength, moisture content or cone penetration resistance.

(3) Perform repeated load tests on actual pavements or crater repairs where the induced rut depth are measured throughout the testing program.

(4) Develop software to implement the initial strain procedure for computing residual displacements.

(5) Compare which constitutive laws, e.g. Hardin, overburden dependent, linear, or hyperbolic, yield the best estimate for the first cycle permanent strains.

REFERENCES

1. Chow, Y. T., Ledbetter, R. H. "The Behavior of Flexible Airfield Pavements Under Loads - Theory and Experiments". Final report, prepared for AFWL, report No. AFWL-TR-72-215, July 1973.

2. Knox, Kenneth J. "Small Crater Expedient Repair Test", Final Report, prepared for Air Force Engineering and Services Center, Report No. ESL-TR-80-42, August 1980.

3. Katona, M. G., Smith, J. M., Odello, R. J., Allgood, J. R. "CANDE - A Modern Approach for the Structural Design and Analysis of Buried Culverts", Civil Engineering Laboratory, Naval Construction Battalion Center, Port Hueme, California, October 1976.

4. Hardin, Bobby O. "Characterization and Use of Shear Stress-Strain Relations for Airfield Subgrade and Base Course Materials", Final report, prepared for A.F.W.L., Report No. AFWL-TR-71-60, June 1971.

5. Hardin, Bobby O. "Effects of Strain Amplitude on the Shear Modulus of Soils", College of Engineering, University of Kentucky, Report no. UKY-TR63072-CE23. November 1972.

6. Harding, Bobby O. "Shear Modulus of Gravels", College of Engineering, University of Kentucky, Report No. UKY-TR74073-CE19, September 1973.

7. Majidzadeh, Kamram, Bayomy, Fouad, and Khedr, Safwan. "Rutting Evaluation of Subgrade Soils in Ohio". TRB, Transportation Research Record G81, pp. 75-84.

8. McLean, D. B., Brooker, E. W., "Estimation of Permanete Deformation in Asphalt Concrete Layers Due to Repeated Traffic Loading", TRB, Transportation Research Record 510, pp. 14-30.

9. Parker, Frazier, Barker, Walter R., Gunkel, Robert C., Odom, Eugene C. "Development of a Structural Design Procedure for Rigid Airport Pavements", Final Report, prepared for DOT, Report No. DOT-FA73WAI-377, April 1979.

10. Rude, Lawrence C. "Evaluation of the Bomb Damage Repair Computer Code", Final Report, prepared for AFOSR, for 1980 USAF-SCEFE Summer Faculty Research Program. Contract No. F49620-79-C-0038, September 1980.

11. Poulsen, Jens. "Laboratory Testing of Cohesive Subgrades: Results and Implications Relative to Structural Pavement Design and Distress Models". TRB, Transportation Research Record 671, pp. 84-91.

12. Sanglerat, G., The Penetrometer and Soil Exploration, New York: Elsevier Scientific Publishing Company, 1972.

13. Selig, Ernest T., Chang, Ching S., Alva-Hurtado, Jorge E. and Adegoke, Clement W. "A Theory for Track Maintenance Life Prediction", Final Report, prepared for USDOT, Report No. DOT-RSPA/DPB-50/81/25, June 1981.

14. Snaith, M. S., McMullen, D., Freer-Hewish, R. J., Shein, A. "Flexible Pavement Analysis", Final Technical Report, prepared for U.S. Army Research, Development and Standardization Group - United Kingdom, Box 65, FPO, N.Y. 09510, Report No. DAERO-78-6-125, May 1980.

15. Turnage, G. W., Brown, D. N. "Prediction of Aircraft Ground Performance by Evaluation of Ground Vehicle Rut Depths", Final Report, prepared for AFWL, Report No. AFWL-TR-73-213, February 1974.

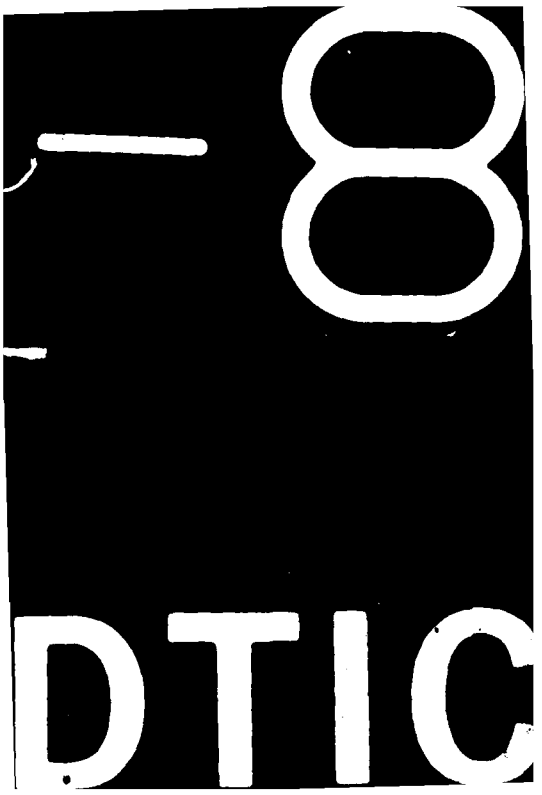
8
DTIC